Optik - International Journal for Light and Electron Optics 183 (2019) 579–585

Contents lists available at ScienceDirect

Optik

journal homepage: www.elsevier.com/locate/ijleo

Original research article

Polarization stabilized VCSELs by displacement Talbot lithography-defined surface gratings☆

Yingying Liu[a,b], Xing Zhang[a,*], Youwen Huang[a,*], Jianwei Zhang[a], Werner Hofmann[c], Yongqiang Ning[a], Lijun Wang[a]

[a] Changchun Institute of Optics, Fine Mechanics and Physics, Chinese Academy of Sciences, Changchun 130033, China
[b] University of Chinese Academy of Sciences, Beijing 100049, China
[c] School of Solid State Physics, Technical University of Berlin, Berlin 10623, Germany

ARTICLE INFO

Keywords:
Vertical cavity surface emitting lasers
Semiconductor lasers
Gratings
Polarization-selective devices

ABSTRACT

Polarization-stable vertical-cavity surface-emitting lasers (VCSELs) with a simple fabrication process are presented. The gratings fixing the polarization are defined by a two-step exposure technology taking advantage of the displacement Talbot lithography technique. This enables grating lines to remain within the inner circle mesa of the VCSELs. These surface grating VCSELs with different periods are theoretically modeled and experimentally verified. Most of these VCSELs exhibit full polarization stability as predicted theoretically. For VCSELs with grating periods larger than the emission wavelength we found a weak orthogonal polarization suppression ratio, thereby deviating from those grating VCSELs with smaller periods.

1. Introduction

Vertical cavity surface emitting lasers (VCSELs) have been gaining increased researchers' attention because of their unique properties [1,2]. However, the lack of a priori defined polarization direction may limit their application in optical sensing, spectroscopy, and measurement, where stable polarization is desirable or even mandatory [3,4]. In the past, considerable work has been performed such as anisotropic gain [5], asymmetric resonators [6,7], external optical feedback [8]. Surface gratings were subsequently proposed. The VCSELs with surface grating directly etched on the mesa performed consistent polarization stability even under strong current modulation [9–16]. High-contrast gratings, as an advanced product of surface gratings, have been incorporated into VCSELs to control their polarization state [17–21]. However, their grating fabrication in laboratory is mostly accomplished by electron beam lithography, which is costly and time consuming. Therefore, the low-cost method of nanoimprint lithography (NIL) was proposed [22,23]. They made the surface gratings to control the polarization for VCSELs by directly pressing the grating mold into the polymer within circular mesa. Whereas, the presence of a residual polymer layer and particulate contamination have been encountered. Displacement Talbot lithography (DTL) is a robust, high-throughput and low-cost technique for patterning nanoscale period structures without contacting the photolithography mask during entire exposure process [24–26].

In this work, we fabricated polarization-stable surface grating VCSELs by a twice exposure technology. The technology takes

☆ Supported by the National Key Research and Development Program (2016YFE0126800); National Natural Science Foundation of China (61434005, 11774343, 11674314, and 61727822); the Science and Technology Program of Jilin Province, China (20180201119GX), the Youth Innovation Promotion Association of China (2017260) and Chinese Academy of Sciences President's International Fellowship Initiative (2018VTA0005).

* Corresponding authors.
E-mail addresses: zhangx@ciomp.ac.cn (X. Zhang), huangyouwen13@mails.ucas.ac.cn (Y. Huang).

https://doi.org/10.1016/j.ijleo.2019.02.139
Received 19 January 2019; Accepted 24 February 2019

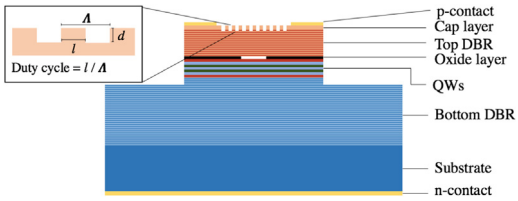

Fig. 1. Grating VCSEL (right) and various grating parameters (left), where Λ is the grating period, d is the grating etch depth, and *l* is the width of the grating ridge.

advantage of a DTL step and an extra ordinary I-line lithograpy step to remain the grating pattern within the inner circle mesa of VCSELs. Firstly, the relative dichroism and optical field of the grating with different periods were theoretically investigated. Then, we fabricated VCSELs without and with different periods gratings to compare their performance. Finally, the polarization characteristics of them were measured and discussed in detail.

2. Device structure and simulation

Fig. 1 shows a schematic cross-section of the VCSEL structure. This grating VCSEL consists of three quantum wells and a one-wavelength (890 nm) inner cavity sandwiched between 34 and 21 pairs of bottom and top distributed Bragg reflectors (DBRs), respectively. A 30 nm-thick high-aluminum-concentration oxide layer is positioned immediately above the active region to provide current and optical confinement. The oxide diameter of VCSELs in this experiment are 5 μm. The diameter of inner circle mesa and outer circle mesa of VCSELs are 10 μm and 20 μm, respectively. The top mirror is terminated by a highly doped GaAs cap layer (50 nm), in which the grating is etched. Grating parameters, such as grating period (Λ), grating etch depth, and duty cycle are marked in Fig. 1.

Because the surface grating introduced different reflectivity, thus threshold gains in parallel and orthogonal orientations. So the polarization-dependent modal loss was first numerical modeled. The threshold gains and relative dichroisms (RDs) were calculated with five grating periods within 100 nm of grating depths. Fig. 2 clearly shows that various etching depths cause different polarization orientations. RD is defined as follows:

$$\mathrm{RD} = 1 - \frac{G_o}{G_p} \tag{1}$$

where G_o and G_p denote the threshold gains of the polarization orientations which orthogonal and parallel to the grating lines, respectively. Positive dichroism means that the polarization of output light is orthogonal to the grating lines, whereas negative dichroism corresponds to polarization parallel to the grating lines. For moderate depths, polarization is perpendicular to the grating lines and switches to another orientation depending on the grating period (e.g., 500 and 700 nm). At 60 nm depth, most periods of the grating VCSELs present positive RDs, which indicates that they are polarized along the same orthogonal orientation, and only the VCSEL with a grating period of 1000 nm yields results that deviate from this trend. Furthermore, its polarization resolution characteristic, which lines close to 0 with all ranges of depth, performs weakly. This issue may be attributed to the diffraction loss problem of the grating integrated above the VCSEL. Therefore, the optical fields of the VCSELs were calculated, as depicted in Fig. 3. The diffraction loss with yellow part in the air above the VCSEL is stronger in the period of 1000 nm than in other periods of the TE part. Simultaneously, the difference between the TE and TM of the optical field with yellow part within the cavity of the VCSEL is the least noticeable.

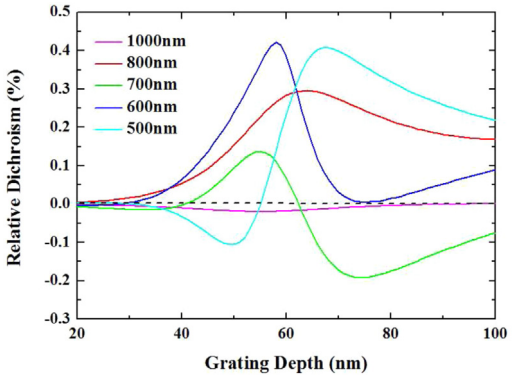

Fig. 2. Calculated RD versus etching depth of gratings with periods of 500 nm, 600 nm, 700 nm, 800 nm, and 1000 nm.

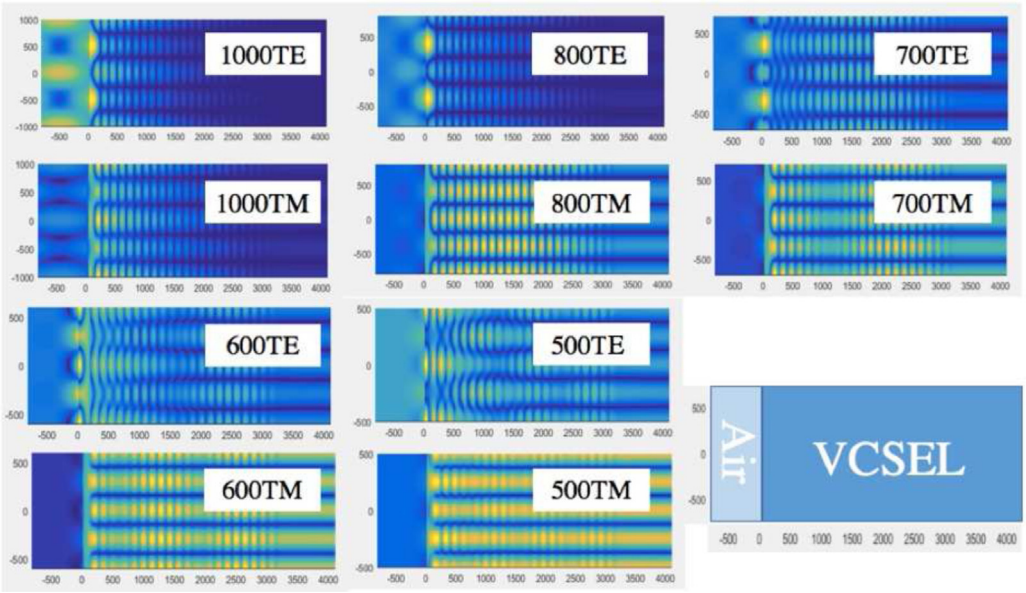

Fig. 3. Optical field calculations of VCSELs with different periods and schematic of a VCSEL.

3. Experiment

The grating in this work was defined using a two-step exposure technology. The DTL technique based on Talbot effect which utilizes monochromatic collimated light projecting into a periodic pattern mask, thus forming self-images at regular distances behind the mask. The regular distance is the Talbot length, approximately $2p^2/\lambda$ where p is the grating period of mask which is twice the grating period on the chip and λ is the project wavelength [24]. When the wafer is placed at an integer multiple of Talbot length, DTL can project refined patterns without contacting the photolithography mask during entire exposure process. Here we set five periods of grating, 500, 600, 700, 800 and 1000 nm. The project wavelength is 377 nm. Accordingly, the Talbot lengths calculated are 5.3, 7.6, 10.3, 13.58 and 21.2 μm, respectively. The gap between wafer and mask was set approximately 30 μm ~ 50 μm at the beginning, but no need to ensure a more precise gap setting. Because, when the exposure begins, the wafer will move up and down, and the exposure just happens when the gap equal to an integer multiple of Talbot length.

Fig. 4 shows the fabrication steps of a wafer with a photoresist on it to grating etched in the cap layer. The top and cross views show that the wafer includes only a cap layer and a top DBR for simplicity. Firstly, DTL was used to achieve the high-resolution periodic pattern. In the first row, the photoresist was spun on the wafer. The second row shows that the DTL lithography can produce only equal-length grating lines whereas the grating lines within the inner circle mesa of a VCSEL are unequal in length. Therefore, a second I-line lithography is introduced to maintain the grating lines within the size of the VCSEL's inner circular mesa. Normal optical lithography could be used to achieve this alignment because the second exposure does not require high resolution. The third row shows the patterns that remained after two step exposure. The surface grating was subsequently dry etched using an inductively coupled plasma (ICP) etcher in the fourth row. The diameter of inner circle mesa and outer circle mesa of VCSELs are 10 μm and 20 μm, respectively. The grating etch depth was 60 nm, and duty cycle was 50%. The proposed grating definition technique that uses the two-step exposure presents many advantages, including low cost, time saving, and suitability for large-volume production. Then, the following step was conducted in the same manner as in common VCSELs, which have no grating. Fig. 5 shows the enlargement of the grating on the out-coupling facet of the VCSEL with five periods, as measured by scanning electron micrograph (SEM) from the top of the devices. The periods are from 500 nm to 1000 nm. The upper surface of fully processed grating VCSEL was also given in the lower right corner.

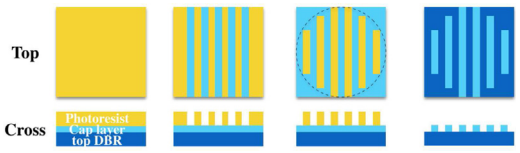

Fig. 4. Fabrication steps of DTL defined gratings.

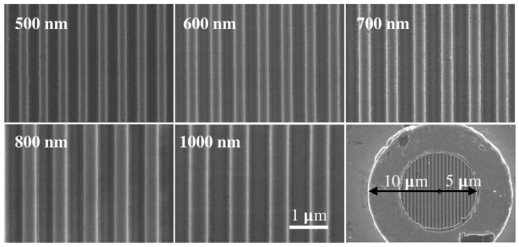

Fig. 5. SEM of the enlargement of surface grating over the out-coupling facet of VCSELs with periods from 500 nm to 1000 nm. The lower right corner is the upper surface of fully processed grating VCSEL. The radius of inner circle mesa and outer circle mesa of VCSELs are 5 μm and 10 μm, respectively.

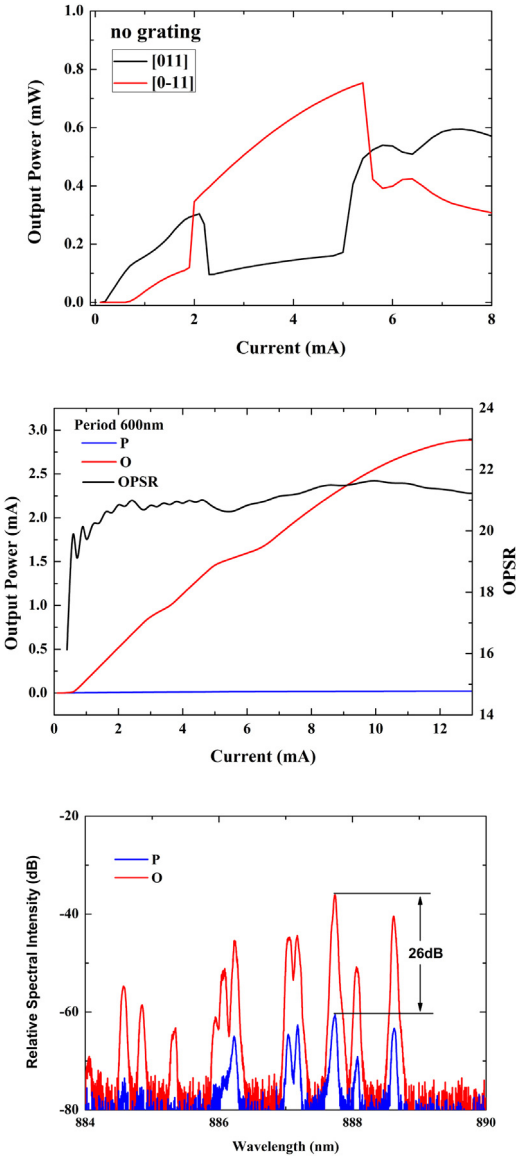

Fig. 6. PR-*LI* characteristics of reference VCSEL without any extra structure (top) and a surface grating VCSEL (center), featuring a grating period of 600 nm. PR-spectra of the grating VCSEL (bottom). P represents the polarization direction parallel to the direction of the grating lines. O represents the polarization direction orthogonally to the direction of the grating lines.

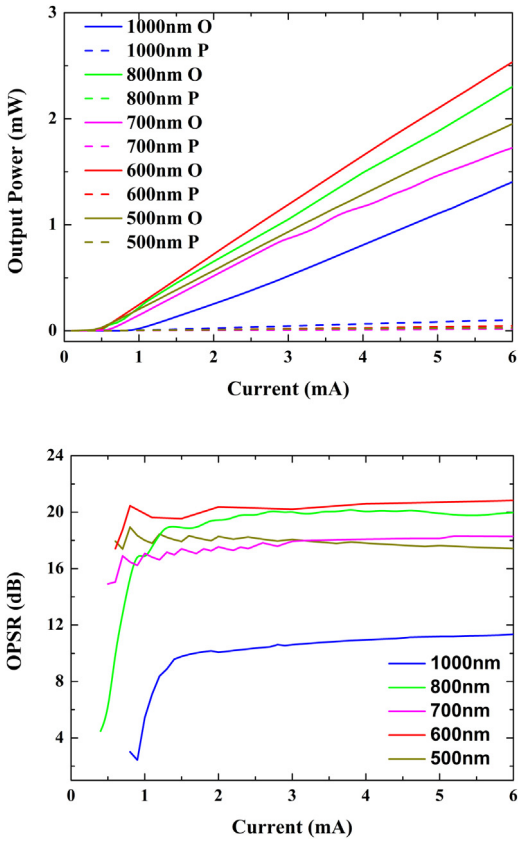

Fig. 7. PR-*LI* characteristics and OPSRs of grating VCSELs in different grating periods.

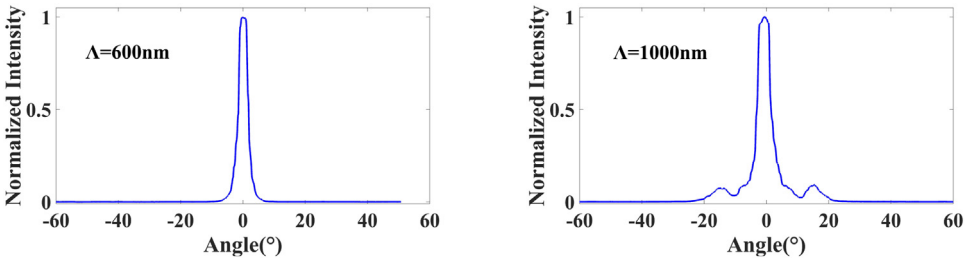

Fig. 8. Far-fields of 6 μm oxide diameter grating VCSELs at periods of 600 and 1000 nm.

4. Results and discussion

The polarization-resolved light-current (PR-*LI*) characteristics and spectra of a reference device and a multimode VCSEL was measured to illustrate the polarization control ability achieved by the fabricated surface gratings. The polarization characteristics of adjacent VCSELs without and with grating lines are shown in Fig. 6. The reference VCSEL with no surface grating begins to lase along the [0 − 11] polarization. At 2 mA, the first polarization switch appears which caused by the first higher-order mode orthogonal to the fundamental one. And a second partial polarization switch comes out at a current of 4.8 mA. At this point, the second mode begins to lase. For high currents, the output power seems to be arbitrarily divided between the two orthogonal polarizations. The PR-*LI* of grating VCSEL is shown in the middle of Fig. 6, the grating period is 600 nm. The orthogonal polarization suppression ratio (OPSR) is calculated by the two polarization powers as

$$\mathrm{OPSR} = 10\log\left(\frac{P_{[0-11]}}{P_{[011]}}\right) \tag{2}$$

and displayed in the middle of Fig. 6. The average OPSR is 21 dB, which is calculated on the basis of the data obtained from the current with a step size of 0.1 mA. The grating VCSEL shows one fixed polarization over the entire current range. This polarization was orthogonal to the grating lines up to the thermal rollover, and the other orientation polarization is strongly suppressed. The

influence of the surface grating on threshold current and output power is not evident. The PR-spectra were measured at 1.5 mA and shown in the bottom part of Fig. 6. The spectra clearly demonstrate the OPSR from the gap between the orthogonal and parallel polarization peak is 26 dB, which is larger than that calculated above. And the difference is originated from spontaneous emission and suppressed modes are also included when the optical powers were measured, inevitably.

Furthermore, surface grating VCSELs with five grating periods were established. The VCSELs featured grating periods of 1000, 800, 700, 600, and 500 nm. The gratings were oriented along the [011] crystallographic axis. All of the VCSELs exhibit well-defined and stable polarization for all grating periods up to the thermal rollover because of the large dichroism introduced by using a dielectric surface grating with the optimized grating parameters described previously. Fig. 7 shows the PR-*LI* characteristics of grating VCSELs with these five periods. The grating VCSELs demonstrate remarkable polarization control, except for the device with the period of 1000 nm which is larger than the VCSEL wavelength of 890 nm. Simultaneously, the threshold current of the grating VCSEL with the period of 1000 nm is larger and its output power is smaller than those of the other devices. The average OPSR of this device is approximately 11 dB, whereas those of the other periods are all above 17 dB. The grating VCSELs with the period of 600 nm perform the excellent polarization characteristics in this experiment. The diffraction loss of grating VCSELs with periods could be intuitively observed with the aid of far-field shown in Fig. 8. The grating periods of 600 nm, as a representative of smaller period than the VCSEL wavelength, and 1000 nm, which is larger than the VCSEL wavelength, were compared. The device with a period of 600 nm emits only at the center lobe, and no emission side lobes appear. However, the side lobes clearly arise in the plot of the large-period-grating VCSEL, and strong side lobes appear in the region of approximately ± 15°. The considerable power of the side lobes may be the cause of the total power to decrease.

5. Conclusion

In summary, a newly defined technology called two-step exposure lithography is proposed to promote efficient and economical mass fabrication of polarization-stable grating VCSELs. The polarization characteristics of grating VCSELs with different periods were investigated in detail theoretically and experimentally. The results show that the VCSELs with grating period shorter than the wavelength exhibited a remarkable OPSR of 17 dB, and the VCSELs with grating period longer than the lasing wavelength show an obvious diffraction and a relatively low OPSR. Therefore, for a further improvement in OPSR, much more attention should be paid to the grating whose period is no more than the lasing wavelength of VCSEL in future production.

References

[1] A. Larsson, Advances in VCSELs for communication and sensing, IEEE J. Sel. Top. Quantum Electron. 17 (6) (2011) 1552–1567, https://doi.org/10.1109/jstqe.2011.2119469.
[2] Y. Mei, G.-E. Weng, B.-P. Zhang, J.-P. Liu, W. Hofmann, L.-Y. Ying, J.-Y. Zhang, Z.-C. Li, H. Yang, H.C. Kuo, Quantum dot vertical-cavity surface-emitting lasers covering the 'green gap', Light Sci. Appl. 6 (1) (2016) e16199, https://doi.org/10.1038/lsa.2016.199.
[3] M. San Miguel, Q. Feng, J. Moloney, Light-polarization dynamics in surface-emitting semiconductor lasers, Phys. Rev. A 52 (2) (1995) 1728–1739, https://doi.org/10.1103/PhysRevA.52.1728.
[4] M.P. Van Exter, v.D.A.K. Jansen, J.P. Woerdman, Electro-optic effect and birefringence in semiconductor vertical-cavity lasers, Phys. Rev. A 56 (1) (1997) 845–853, https://doi.org/10.1103/PhysRevA.56.845.
[5] A. Mizutani, N. Hatori, N. Nishiyama, F. Koyama, K. Iga, A low-threshold polarization-controlled vertical-cavity surface-emitting laser grown on GaAs (311)B substrate, IEEE Photonics Technol. Lett. 10 (5) (1998) 633–635, https://doi.org/10.1109/68.669216.
[6] C.L. Chua, R.L. Thornton, D.W. Treat, R.M. Donaldson, Anisotropic apertures for polarization-stable laterally oxidized vertical-cavity lasers, Appl. Phys. Lett. 73 (12) (1998) 1631–1633, https://doi.org/10.1063/1.122228.
[7] S. Riyopoulos, E. Nhan, Polarization selection due to scattering losses in nonaxisymmetric vertical cavity surface emitting laser cavities, Appl. Phys. Lett. 85 (15) (2004) 3038–3040, https://doi.org/10.1063/1.1799239.
[8] M.A. Arteaga, O. Parriaux, H. Thienpont, K. Panajotov, Polarized optical feedback from an extremely short external cavity for controlling and stabilizing the polarization of vertical cavity surface emitting lasers, Appl. Phys. Lett. 90 (12) (2007) 1402, https://doi.org/10.1063/1.2714301.
[9] D.S. Song, S.H. Kim, H.G. Park, C.K. Kim, Y.H. Lee, Single-fundamental-mode photonic-crystal vertical-cavity surface-emitting lasers, Appl. Phys. Lett. 80 (21) (2002) 3901–3903, https://doi.org/10.1063/1.1481984.
[10] J.M. Ostermann, P. Debernardi, C. Jalics, R. Michalzik, Polarization-stable oxide-confined VCSELs with enhanced single-mode output power via monolithically integrated inverted grating reliefs, IEEE J. Sel. Top. Quantum Electron. 11 (5) (2005) 982–989, https://doi.org/10.1109/jstqe.2005.854145.
[11] P. Debernardi, J.M. Ostermann, M. Feneberg, C. Jalics, R. Michalzik, Reliable polarization control of VCSELs through monolithically integrated surface gratings: a comparative theoretical and experimental study, IEEE J. Sel. Top. Quantum Electron. 11 (1) (2005) 107–116, https://doi.org/10.1109/jstqe.2004.841712.
[12] A. Haglund, J.S. Gustavsson, J. Bengtsson, P. Jedrasik, A. Larsson, Design and evaluation of fundamental-mode and polarization-stabilized VCSELs with a subwavelength surface grating, IEEE J. Quantum Electron. 42 (3) (2006) 231–240, https://doi.org/10.1109/jqe.2005.863703.
[13] J.M. Ostermann, P. Debernardi, R. Michalzik, Optimized integrated surface grating design for polarization-stable VCSELs, IEEE J. Quantum Electron. 42 (7) (2006) 690–698, https://doi.org/10.1109/jqe.2006.876721.
[14] A. Al-Samaneh, M.T. Haidar, D. Wahl, R. Michalzik, Polarization-stable single-mode VCSELs for Cs-based miniature atomic clocks, CLEO EUROPE/EQEC, IEEE, 2011, p. 1, https://doi.org/10.1109/cleoe.2011.5942632.
[15] M.J. Miah, A. Al-Samaneh, A. Kern, D. Wahl, P. Debernardi, R. Michalzik, Fabrication and characterization of low-threshold polarization-stable VCSELs for Cs-based miniaturized atomic clocks, IEEE J. Sel. Top. Quantum Electron. 19 (4) (2013) 1701410, https://doi.org/10.1109/JSTQE.2013.2247697.
[16] X. Zhang, B. Liu, K. Shi, F. Han, H. Chen, L. Nie, X. Yu, A thermal analysis of stable-polarization VCSELs, Optik 157 (2018) 203–207, https://doi.org/10.1016/j.ijleo.2017.11.091.
[17] M.C.Y. Huang, Y. Zhou, C.J. Chang-Hasnain, A surface-emitting laser incorporating a high-index-contrast subwavelength grating, Nat. Photonics 1 (2) (2007) 119–122, https://doi.org/10.1038/nphoton.2007.73.
[18] M.C.Y. Huang, Y. Zhou, C.J. Chang-Hasnain, Polarization mode control in high contrast subwavelength grating VCSEL, CLEO/QELS, IEEE, 2008, pp. 1–2, https://doi.org/10.1109/cleo.2008.4551186.
[19] R. Michalzik, VCSELs: A Research Review, Springer Berlin Heidelberg, 2013, https://doi.org/10.1007/978-3-642-24986-0_1.
[20] P. Qiao, K. Li, K.T. Cook, C.J. Chang-Hasnain, MEMS-tunable VCSELs using 2D high-contrast gratings, Opt. Lett. 42 (4) (2017) 823, https://doi.org/10.1364/OL.42.000823.
[21] J.M. Ostermann, P. Debernardi, R. Michalzik, Optimization of polarization-stable single- and multi-mode surface grating VCSELs towards high fabrication

tolerance and superior performance, in: D. Lenstra, M. Pessa, I.H. White (Eds.), Photonics Europe, SPIE, 2006, pp. 618410–618412, , https://doi.org/10.1117/12.661632.
[22] M.A. Verschuuren, P. Gerlach, H.A. van Sprang, A. Polman, Improved performance of polarization-stable VCSELs by monolithic sub-wavelength gratings produced by soft nano-imprint lithography, Nanotechnology 22 (50) (2011) 505201–505210, https://doi.org/10.1088/0957-4484/22/50/505201.
[23] S. Inoue, J. Kashino, A. Matsutani, H. Ohtsuki, T. Miyashita, F. Koyama, Highly angular dependent high-contrast grating mirror and its application for transverse-mode control of VCSELs, Jpn. J. Appl. Phys. 53 (9) (2014) 090306, https://doi.org/10.7567/JJAP.53.090306.
[24] H.H. Solak, C. Dais, F. Clube, Displacement Talbot lithography: a new method for high-resolution patterning of large areas, Opt. Express 19 (11) (2011) 10686–10691, https://doi.org/10.1364/OE.19.010686.
[25] H.H. Solak, C. Dais, F. Clube, L. Wang, Phase shifting masks in Displacement Talbot Lithography for printing nano-grids and periodic motifs, Microelectron. Eng. 143 (C) (2015) 74–80, https://doi.org/10.1016/j.mee.2015.03.050.
[26] L. Wang, F. Clube, C. Dais, H.H. Solak, J. Gobrecht, Sub-wavelength printing in the deep ultra-violet region using Displacement Talbot Lithography, Microelectron. Eng. 161 (2016) 104–108, https://doi.org/10.1016/j.mee.2016.04.017.